

ORIGINAL ARTICLE

Preparation and evaluation of solid dispersions of piroxicam and Eudragit S100 by spherical crystallization technique

Maryam Maghsoodi and Fatemeh Sadeghpour

Drug Applied Research Center and School of Pharmacy, Tabriz University of Medical Sciences, Tabriz, Iran

Abstract

Objective: To improve the dissolution rate of piroxicam (PX), enteric-release microparticles having solid dispersion (SD) structure were prepared in one step. **Methods:** SD of PX and Eudragit S100 (Eu S100) with the aid of silicon dioxide (Aerosil® 200), as an antiadhesion agent, were prepared by spherical crystallization technique. The microparticles were characterized by differential scanning calorimetry, X-ray powder diffraction, and Fourier transform infrared spectroscopy and were evaluated for yield, encapsulation efficiency, flowability, packability, and drug release (at pH 1.2 and pH 7.4). The samples were stored at severe condition [40°C, 75% relative humidity (RH)] for 3 months to investigate their stability. The effects of the polymer–drug and polymer–Aerosil ratios on the characteristics of the microparticles were also investigated. **Results:** PX microparticles exhibited significantly improved micromeritic properties in comparison to the crystalline pure drug. The dissolution of drug from microparticles in phosphate buffer (pH 7.4) indicated a significant increase in dissolution of PX when dispersed in Eu S100. The results of X-ray powder diffraction and differential scanning calorimetry analysis indicated that in microparticles at 2:1 Eu S100:PX ratio the crystalline form of PX was disordered, suggesting that PX was highly dispersed in microparticles, as that in the amorphous state. Fourier transform infrared spectroscopy analysis demonstrated the presence of intermolecular hydrogen bonding between PX and Eu S100 in SD. In stability test, the release profiles of the microparticles were unchanged as compared with the freshly prepared SDs; amorphous PX in the SD particles did not crystallize under storing at 40°C, 75% RH for 3 months.

Key words: Aerosil; enteric microparticles; Eudragit S100; piroxicam; spherical crystallization

Introduction

Piroxicam (PX) is a potent nonsteroidal anti-inflammatory drug used for its analgesic, antipyretic, and anti-inflammatory properties in humans¹ and small animals^{2,3}. According to the Biopharmaceutical Classification System PX is regarded as a class II compound characterized by a low water solubility. Drug release is a crucial and a limiting step for oral drug bioavailability, particularly for drugs with low gastrointestinal solubility and high permeability. By improving the drug release profile of these drugs, it is possible to enhance their bioavailability and reduce side effects^{4–8}.

Irritation of the gastrointestinal tract is, as with most nonsteroidal anti-inflammatory drugs, one of the major side effects reported after oral administration of PX^{1,9}. As

its gastrointestinal intolerance is not only related to the inhibition of the prostaglandin synthesis but also to acute local contact of the drug with the gastric mucosa¹⁰, the development of an enteric multiparticulate drug delivery system might reduce or even avoid the mucosal irritation.

The solid dispersions (SDs) technique for water-insoluble drugs was one of the efficient methods to improve the dissolution rate¹¹. SD of PX with enteric polymers offers the additional advantages of increasing the in vivo absorption rate as well as reducing the acute gastric damage. During the past 40 years, there has been a great deal of interest in the pharmaceutical field in using SDs to improve the bioavailability for poorly water-soluble drugs^{12–15}. SD techniques commonly used were dissolution method, fusion method, fusion–dissolution method, and so on. Manufacturing

Address for correspondence: Dr. Maryam Maghsoodi, Drug Applied Research Center and School of Pharmacy, Tabriz University of Medical Sciences, Tabriz 51664, Iran. Tel: +98 411 3392593, Fax: +98 411 3344798. E-mail: maghsoodim@tbzmed.ac.ir

(Received 8 Jul 2009; accepted 23 Dec 2009)

processes of a SD system are usually composed of several steps, that is, firstly, drug being deposited on SD carries, then the solid dispersed product being crushed, sieved and mixed with other excipients, and being granulated for tableting or filling into capsules. Sometimes, resultant products have to be coated with suitable materials for controlling the drug release. Therefore, careful control of each step should be required to produce reproducible and reliable preparation.

The spherical crystallization technique has been developed as an efficient particle design technique for 20 years¹⁶. This technique has been successfully utilized for improvement of flowability and compactibility of crystalline drugs^{17,18}. Moreover, polymers were introduced in system to prepare functional drug device such as microparticles^{19,20}, microcapsules²¹, microballoons²², and biodegradable nanospheres²³, in which the crystals of drug and polymers were coprecipitated and directly agglomerated into spherical forms²⁴. Further application of this technique to produce a SD system with water-insoluble drug to improve bioavailability has been desired to develop simple preparation processes²⁵.

The main purpose of this study is to improve dissolution rate of PX by preparation of microparticles and the SD in one step.

Materials and methods

Materials

PX (Shasun Chemicals & Drugs, Pondicherry, India), Eudragit S100 (Eu S100) (MW~135 KDa; Röhm GmbH, Darmstadt, Germany), Aerosil® 200 (Ae) (Mingtai Chemical, Taiwan, China), polyvinyl alcohol (PVA) (MW ~ 70 kDa, 88% hydrolyzed; Sigma, Deisenhofen, Germany), and ethanol and dichloromethane (Merck, Darmstadt, Germany) were used. The solvents were of analytical grade.

Preparation of the microparticles

PX (0.1–0.6 g) was dissolved with Eu S100 (0.6 g) in a mixed solution of ethanol (good solvent, 5 mL) and dichloromethane (bridging liquid, 5 mL) at 35°C. Then Ae (0.15–0.3 g) was added to the drug-polymer solution and magnetically stirred (600 rpm) to obtain a uniform suspension. The microparticles were prepared by immediately adding the resultant drug-polymer-Ae suspension to 200 mL distilled water containing 0.25% of PVA (at 25°C) placed in a cylindrical vessel (500 mL) equipped with three baffles under agitation (400 rpm) using a propeller-type stirrer with four blades (each blade is 17 × 18 mm). After agitating the system for 20 minutes the solidified microparticles were recovered by filtration. The resultant products were dried in an oven at 50°C for 6 hours.

Determination of production yield and encapsulation efficiency of microparticles

All microparticle formulations were prepared in triplicate. Microparticles dried at 50°C were then weighed and the yield of microparticle preparation was calculated using the formula

$$\text{Production yield(\%)} = \frac{\text{practical mass (microparticles)}}{\text{theoretical mass (polymer + drug + Aerosil)}} \times 100. \quad (1)$$

Microparticles were crushed and powdered by using a mortar. Accurately weighed 20 mg of this powder was extracted in 20 mL of ethanol. The solution was then filtered, a sample of 2 mL was withdrawn from this solution and assayed spectrophotometrically to determine the PX content of the microparticles. A calibration curve based on standard solutions of PX in ethanol was used to calculate the PX concentration.

The encapsulation efficiency (%) was calculated using Equation (2).

$$\text{Encapsulation efficiency(\%)} = \left(\frac{M_{\text{actual}}}{M_{\text{theoretical}}} \right) \times 100, \quad (2)$$

where M_{actual} is the actual PX content in weighed quantity of powder of microparticles and $M_{\text{theoretical}}$ is the theoretical amount of PX in microparticles calculated from the quantity added in the fabrication process. The means of three assays were reported.

Measurement of micromeritic properties

Size distribution and mean diameter were determined using the sieving method. A total of 25 g of material was sieved using an Erweka vibration sieve (Erweka, Heusenstamm, Germany) through a nest of sieves (mesh numbers 20, 25, 30, 35, 40, 45, 50, 60, 70, 80, 100, and 120). The vibration rate was set at 200 strokes/min, and the sieving time was 10 minutes. The powder fractions retained by the individual sieves were determined and expressed as mass percentages. The morphology of the microparticles was observed by optical microscopy (Nikon Labophot, Tokyo, Japan).

Flowability of the crystals was assessed by determining the angle of repose and the compressibility index (Carr index, CI). The angle of repose was measured by a fixed funnel method²⁶. The CI^{27,28} is a measure of the propensity of a powder to consolidate. Changes occurring in packing arrangement during the tapping procedure are expressed as the CI (Equation 3).

$$CI = \frac{(\text{tapped density} - \text{bulk density})}{\text{tapped density}} \times 100. \quad (3)$$

The CI reflects the packability of the powders, and there is also a correlation between the CI and the flowability of the crystals. The results presented are mean value of six determinations.

Differential scanning calorimetry

The thermal characteristics of the microparticles and pure drug were determined using a differential scanning calorimeter (DSC60, Shimadzu, Japan). After calibration with indium and lead standards, samples of the crystals (3–5 mg) were heated (range 25–300°C) at 10°C/min in hermetically sealed aluminum pans.

X-ray powder diffraction

To investigate polymorphism X-ray was used. The cavity of the metal sample holder of the X-ray diffractometer was filled with the ground sample powder and then smoothed with a spatula. X-ray diffraction pattern of PX samples was obtained using the X-ray diffractometer (Model D5000; Siemens, Hamburg, Germany) at 40 kV, 30 mA, and a scanning rate of 0.06°/min over the range $2\theta = 5\text{--}40$, using $\text{CuK}\alpha 1$ radiation of wavelength 1.5405Å.

FTIR spectroscopy

Infrared spectra were recorded using a Fourier transform infrared spectroscopy (FTIR) spectrophotometer (M-B-100; Bomem, Quebec, Canada) utilizing potassium bromide discs. Samples were prepared by gently grounding the powder with KBr. The data region was 4000–1000 cm^{-1} .

In vitro release studies

The in vitro dissolution of PX as pure drug and microparticles was determined with a USP rotating paddle method (900 mL 0.1 N HCl or pH 7.4 phosphate buffer, 100 rpm, 37°C, $n = 3$). At preset time intervals aliquots were withdrawn and replaced by an equal volume of dissolution medium to maintain constant volume. After suitable dilution, the samples were analyzed spectrophotometrically at 333.2 and 349.2 nm for the 0.1 N HCl and pH 7.4 phosphate buffer, respectively.

Stability studies

A 3-month accelerating condition stability test was carried out after preparation by which the microparticles were kept in a desiccator at a temperature of 40°C and a

RH of 75%. To evaluate the stability of the microparticles, in vitro dissolution tests and differential scanning calorimetry (DSC) analysis were performed on the samples.

Statistical analysis

Statistical data analysis was performed using the Student's *t*-test or analysis of variance with $P < 0.05$ as the minimal level of significance.

Results

When the resultant mixed solution of ethanol (good solvent) and dichloromethane (bridging liquid) containing drug, polymer, and Ae was poured into water (poor solvent) under stirring, finely dispersed droplets were formed immediately, and semitransparent emulsion was observed visually. With the diffusion of the good solvent out of the droplets into the poor solvent, the drug, and the polymer coprecipitated in the droplets. The dichloromethane mixed into the good solvent; bridged the drug, Ae, and polymer in the droplets; and the droplets solidified gradually into microparticles. The formation of microparticles could be described in the following processes: the formation of quasi-emulsion droplets, the diffusion of the organic solvent, and the solidification of the droplets. In previous researches^{29,30} for the preparation of microparticles with methacrylic copolymer (Eu L100, S100, RS, and RL) using spherical crystallization technique (quasi-emulsion solvent diffusion method), a large ratio of drug to Eu (>4/1) and also a large amount of organic solvent had to be used, as the polymer revealed a high viscosity during the formation of droplets, and the resulting droplets often agglomerated into an irregular mass and adhered to the propeller or the vessel wall. In this study, however, these problems could be avoided effectively because of the good antiadhesion property of Ae. During the preparation process of microparticles, Ae mixed with the polymer uniformly. A decrease in viscosity prevented conglutination between the emulsified droplets. Ae is a good antiadhesion agent against the viscous characteristic of polymers. At the same time, it could accelerate the solidification of droplets and be packed in the microparticles well. It was also found that introducing proper amount of additives into the distilled water was a favorable method to prevent coalescence of the droplets. In this study, the distilled water containing PVA (0.25%, w/v) was selected as a poor solvent and spherical microparticles of PX were prepared successfully as seen in Figure 1. The microparticles were invariably spherical, although the plasticizer was not added in this formulation. It was indicated that Eu S100 was one of the suitable polymers for the preparation of microparticles using this method because of its good plastic deformation property.

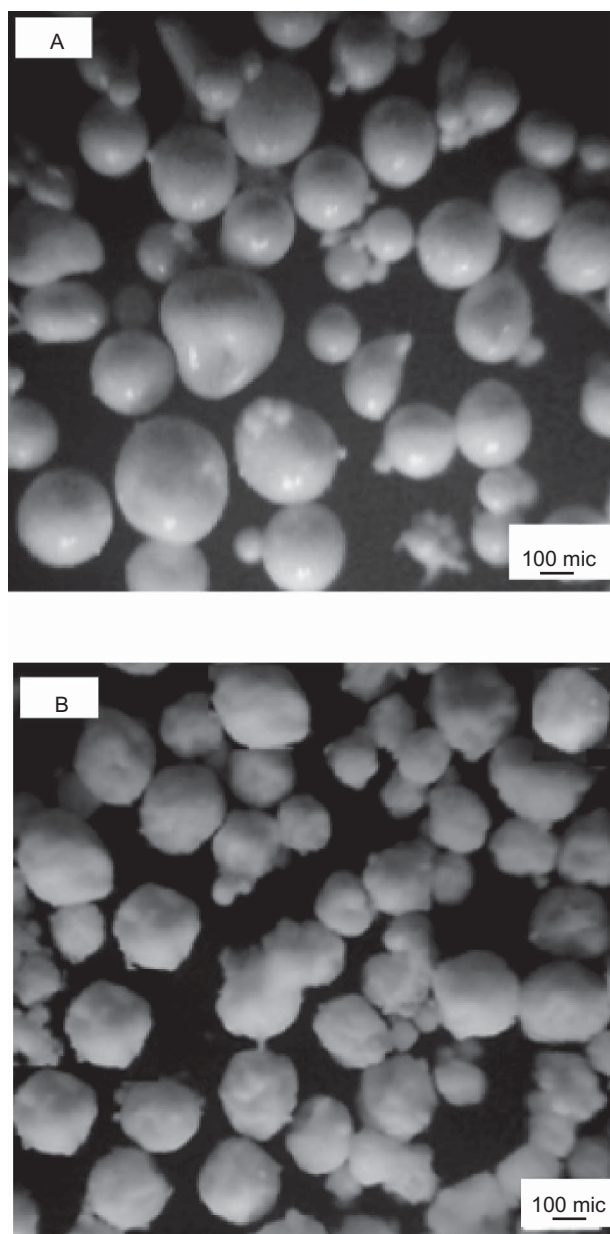


Figure 1. Particle morphology of microparticles (A) Eu S100:PX (2:1) and (B) Eu S100:PX:Ae (2:1:1).

Yield and encapsulation efficiency results

The yields of the microparticles preparation and PX encapsulation efficiencies were high for the microparticles obtained and were affected by the polymer:drug and polymer:Ae ratios (Table 1). Lower yield of Eu:PX microparticles in comparison with Eu:PX:Ae microparticles ($P < 0.05$) may be due to high viscosity of polymer in absence of Ae, which resulted in agglomeration of droplets and adherence to the vessel wall and propeller. Moreover, a fast solidification rate of microparticles in presence of Ae may reduce partitioning of drug and polymer into the external phase of the emulsion.

Losses for the relatively insoluble PX may be because of some dissolution prior to drop formation or during the hardening process³¹. According to this fact, we suppose that any factor that could modify the time needed to reach the physical state-transition boundaries of the polymeric solution (solution-gel-glass) during the hardening process will be effective in the polymer precipitation and consequently in encapsulation efficiency results²⁹. The polymer-to-drug ratio can be a critical factor during microparticle formation. With more polymer:drug ratios, higher encapsulation efficiencies were produced. For instance, PX encapsulation efficiency was increased from 90.8% to 98.3% as polymer:drug ratio was increased from 1:1 to 6:1. This could be because of the changes in viscosity resulting from increasing polymer ratio, which leads to more viscous internal phases and consequently faster solidification rate. Therefore, the microparticle structure is more fixed and thus solvent and nonsolvent counter-diffusion is delayed. As a consequence, less water may be allowed to diffuse into the dispersed phase and less drug will be carried by the solvent into the aqueous phase²⁹. As results showed, inclusion of Ae in the microparticles increased encapsulation efficiency ($P < 0.05$), which may be attributed to faster solidification and, consequently, lower loss of drug before fixation of microparticles structure in the presence of Ae as discussed above. The high encapsulation efficiency of PX in microparticles was believed to be due to the poor solubility of drug in poor solvent. These suggested that this method was

Table 1. Mean diameter, angle of repose, Carr index, yield, and encapsulation efficiency of samples.

	Samples	Mean diameter $\pm \sigma$ (μm)	Angle of repose ($^\circ$)	Carr index (%)	Yield (%)	Encapsulation efficiency (%)
Eu:PX	Untreated PX	10.75 ± 0.36	35.8 ± 1.3	32.3 ± 0.6	—	—
	1:1	250 ± 110	17.3 ± 0.9	7.4 ± 0.2	73.8 ± 1.5	90.8 ± 0.5
	2:1	290 ± 80	20.7 ± 1.0	10.8 ± 0.3	70.6 ± 1.7	92.5 ± 0.6
	4:1	310 ± 260	19.1 ± 1.5	9.1 ± 0.1	71.8 ± 0.9	95.4 ± 0.4
	6:1	380 ± 220	23.2 ± 0.6	11.6 ± 0.3	69.5 ± 1.5	98.3 ± 0.4
Eu:PX:Ae	2:1:1	280 ± 40	24.3 ± 0.5	11.9 ± 0.2	86.9 ± 0.8	96.2 ± 0.4
	4:1:2	322 ± 180	22.6 ± 0.6	10.8 ± 0.3	88.2 ± 0.9	98.2 ± 0.3

suitable for the preparation of microparticles of a poorly water-soluble drug such as PX.

Micromeritic properties

Observations by optical microscopy show that the Eu S100:PX microparticles exhibited spherical morphology and smooth surfaces (Figure 1a) whereas the addition of Ae caused a rather shriveled surface (Figure 1b). As mentioned previously, three processes must be taken into account to explain the formation of the microparticles: the formation of emulsion droplets, the diffusion of the organic solvent, and the solidification of the droplets. When the drug-polymer solution was poured into the poor solvent, the finely dispersed emulsion droplets were formed immediately. Gradually, the emulsion droplets solidified along with diffusion of the good solvent out of the droplets into poor solvent.

Morphology of Eu S100:PX:Ae microparticles might be attributed to fast solidification of membrane on the emulsion droplets periphery in the presence of Ae and afterward loss of internal volume as a result of solvent diffusion. This phenomenon is frequently encountered in the spray drying process. Drug crystals were not observed visually in all microparticles. The particle sizes of microparticles were listed in Table 1. The mean diameter of the microparticles was found to be influenced by the Eu S100:PX ratio.

According to results, larger particles were obtained at higher Eu S100:PX ratios. Increasing the polymer load leads to a more viscous solution, and when the viscous polymeric solution is poured into the aqueous phase, larger droplets and thus larger microparticles are formed³¹⁻³³. On the other hand, an increased solidification rate because of increasing polymer:drug ratio would also tend to reduce the time available for subdivision of larger globules into smaller ones during stirring³⁴. Results showed that inclusion of Ae in microparticles had no significant effect on mean diameter of the microparticles ($P > 0.05$). Table 1 also shows the flowability and packability of the microparticles that were represented in terms of the angle of repose and Carr's index. All microparticles showed excellent flowability and packability (angle of repose, 17-24°; Carr's index, 7-11%). The improved flowability of the microparticles may be because of good sphericity and large size of the microparticles.

During the tapping process, smaller microparticles might have infiltrated into the voids between larger particles, which could result in improved packability (lower CI). These results suggest that the microparticles might be suitable for capsule filling and the capsules formed from them would attain uniformity in weight because of their very good flowability and packability of the microparticles.

DSC and powder X-ray studies

In Figure 2 DSC thermal behaviors of crystalline PX, Eu S100, the microparticles at 1:1 and 2:1 Eu S100:PX ratios, physical mixture of Eu S100:PX at 2:1 ratio, and microparticles at 1:2:1 Eu S100:PX:Ae ratio are reported. PX thermogram showed a melting endothermic peak at 202°C followed by a large peak at 250°C that could be attributed to oxidative decomposition³⁵.

As shown in Figure 2, the melting peak of PX in the microparticles disappeared with increasing the ratio of Eu S100:drug in formulation from 1:1 to 2:1, although the melting peak was observed in the physical mixtures of the Eu S100 and PX at 2:1 ratio. The disappearance of the drug endothermic peak in these microparticles suggested that PX in the microparticles was molecularly dispersed in an amorphous state.

In contrast to pure PX, fusion of PX for physical mixtures of Eu S100:drug (2:1) and microparticles with Eu S100:PX (1:1) occurred in the range of 185-200°C; the final temperature was lower than PX melting point. This indicated a PX:Eu S100 solid-state interaction induced by heating. This type of interaction was previously observed in the physical mixture of PX:PVP K17³⁶.

The XRD patterns of PX, microparticles at 2:1 and 1:1 Eu S100:PX ratios, and microparticles at 1:2:1 Eu S100:PX:Ae were shown in Figure 3. DSC results were further supported by the X-ray analysis, which shows the representative diffraction patterns for the pure PX and the microparticles at 1:1 polymer:drug ratio and no crystalline peaks of PX were found in the microparticles at 2:1 polymer:drug ratio.

Characteristic peaks of PX appeared at a diffraction angle of 2θ , at 8.99°, 15.76°, 23.02°, and 25.85°. These

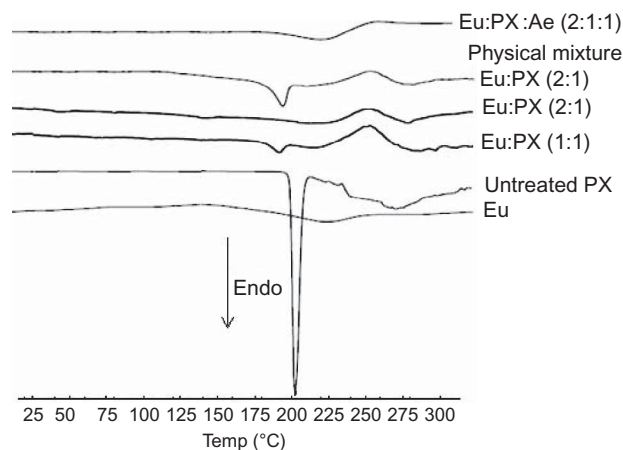


Figure 2. DSC scans of untreated PX, Eu S100, microparticles at Eu S100:PX ratios of 1:1, 2:1, physical mixture of Eu S100:PX (2:1), and microparticles at Eu S100:PX:Ae 2:1:1 ratio.

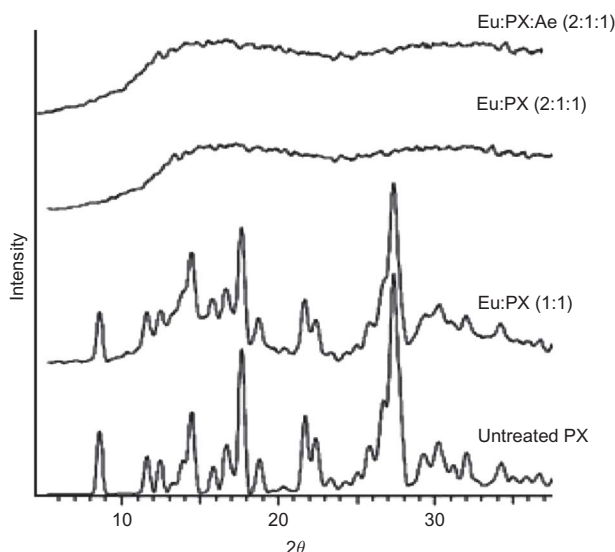


Figure 3. The X-ray diffraction patterns of untreated PX, microparticles at Eu S100:PX ratios of 1:1 and 2:1 and microparticles at Eu S100:PX:Ae 2:1:1 ratio.

values were comparable to those reported for form I of PX^{37,38}.

The XRD peaks of crystalline PX in the microparticles at 1:1 polymer to drug ratio was similar to those in pure drug, indicating that the crystalline form of PX did not change in the microparticles at that ratio. Addition of Ae in microparticle formulations did not change the DSC scans and X-ray powder diffraction patterns as shown in Figures 2 and 3.

FTIR spectroscopy

FTIR spectroscopy was employed to study the interaction in microparticles between PX and Eu S100 (Figure 4). In the IR spectrum of Eu S100, the C = O vibration band of the carboxylic groups presents as a shoulder at 1705 cm^{-1} ; whereas the peak at 1730 cm^{-1} is attributed to the esterified carboxyl groups³⁹.

PX, which is present as enol or zwitterionic forms, showed the N-H or O-H stretching vibration at 3338 cm^{-1} . This region of interest showed the evidence of the interaction between PX and Eu S100 via intermolecular hydrogen bonding between the C=O functions on Eu S100 with the amide (N-H) group or protonated pyridine N atom of PX. The FTIR spectrum of the physical mixture of Eu S100:PX at 2:1 ratio was similar to the synthetic spectra produced by the addition of PX and Eu S100. This indicated that physical mixture spectra were only the summation of PX and Eu S100 spectra and reflected that there was no interaction between PX and Eu S100 in physical mixtures. As shown in Figure 4, the microparticles of Eu S100:PX 1:1 showed peaks of N-H

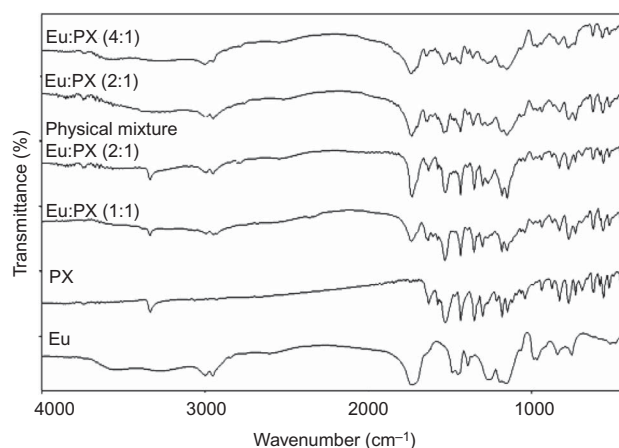


Figure 4. FTIR spectra of untreated PX, Eu S100, microparticles at Eu S100:PX ratios of 1:1, 2:1, 4:1, and physical mixture of Eu S100:PX (2:1).

or O-H stretching vibration of PX at 3338 cm^{-1} despite a broad peak from Eu S100 in this region, whereas the N-H or O-H stretching vibration was not detected in the microparticles of Eu S100:PX at 2:1 and 4:1 ratios that are X-ray amorphous. This might be attributed to a solid-state hydrogen-bonding interaction between amorphous PX and Eu S100 in the microparticles. The intermolecular hydrogen bonding that occurred in amorphous SDs might be stronger than those containing crystalline drug; therefore the N-H or O-H stretching might be weakened resulting in a weak and broad peak that was completely covered by broad peak from Eu S100 in this region^{36,40}.

In vitro release

To evaluate the pH-dependent release profiles of PX from the samples, in vitro release tests were performed under sink condition in 0.1 N HCl and pH 7.4 phosphate buffers. In the dissolution medium at pH 1.2, the pure PX showed a faster drug release (54% within 60 minutes) in comparison with the microparticles (less than 5% in 60 minutes) (Figure 5).

As polymer is insoluble in release media with pH 1.2, microparticles were only slightly swollen and remained intact in this pH, which results in a slow dissolution rate of drug from the microparticles. Whereas at a pH of 7.4, the polymer dissolved rapidly and the microparticles disintegration resulted in a faster drug release rate compared with pH 1.2, as expected.

At a pH of 7.4, the polymer dissolved rapidly and the microparticles disintegration resulted in a faster drug release rate compared with pH 1.2. It can be seen that incorporation of PX into the anionic polymer Eu S100 led to an improvement of the dissolution rate of the

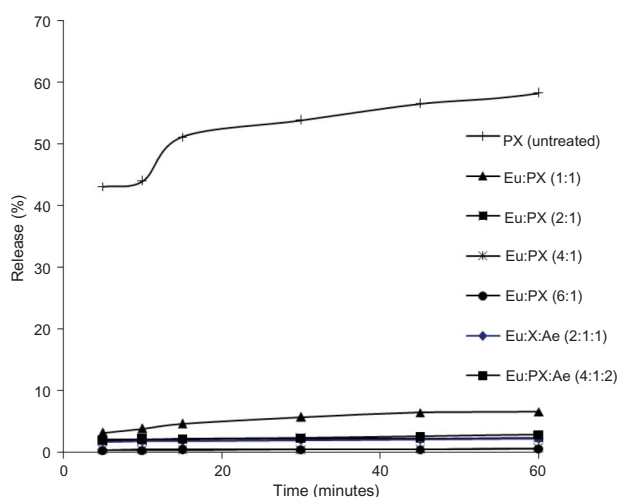


Figure 5. Release of PX from microparticles into 0.1 N HCl (\pm SD, $n = 3$).

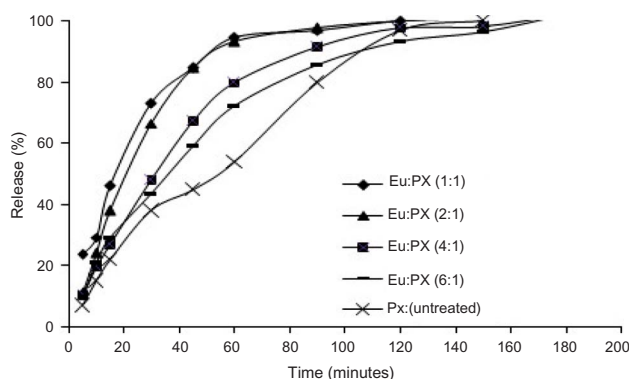


Figure 6. Release of PX from Eu S100:PX microparticles into pH 7.4 phosphate buffer (\pm SD, $n = 3$).

drug at pH = 7.4. This improvement in the drug release might be due to improved wettability of the drug particles^{6,41}, preventing drug aggregation³⁶, significant reduction in particle size during the formation of SDs, or inherently higher rate of dissolution of polymer, which would pull along the more insoluble but finely mixed drug into the dissolution medium^{42,43}.

Interestingly, amorphous dispersion prepared with Eu S100:PX 2:1 has almost equally fast dissolution rate to nonamorphous dispersion of Eu S100:PX 1:1 (Figure 6). To explain this result, the dissolution processes and factors involving dissolution rate would be considered. In general, dissolution may be described by two rate processes: the rate of the interfacial or solid-solvent reaction leading to solubilization of the molecule and the rate associated with the diffusional or transport process of the solvated molecule to the bulk of the dissolution medium.

The dissolution rate of drug is related to many factors. According to Noyes and Whitney equation

$$\frac{dm}{dt} = \frac{DA(Cs - C)}{h},$$

where the rate of change of mass dissolved (m) with time (t) is governed by diffusion coefficient (D), surface area (A) of the solid, thickness of the diffusion layer (h), solubility of the solid (C_s), and concentration of solute in the bulk solution at time t (C). From the Stokes-Einstein equation, the diffusion coefficient is inversely proportional to viscosity. During the process of solubilization, a stagnant layer that surrounds the particle is saturated with dissolved Eu S100 and drug molecules. With the high viscosity of Eu S100 (MW = 135,000 Da), the diffusion coefficient is largely decreased resulting in the low dissolution rate of drug even though the solubilization process can occur fast for the high-energy amorphous form of drug. According to Figure 6, the release rate of the drug from the microparticles was decreased consistently with increasing ratio of Eu S100:PX from 2:1 to 6:1. The increase in the amount of polymer may prevent drug aggregation or the increase in drug wettability resulting in higher solubility. However, the solubilization process might be neutralized by the diffusion process by increasing the viscosity of the solution around the solid particle as discussed above. Therefore, it can be said that the mechanism of dissolution of SD in Eu S100 might be predominantly diffusion-controlled, and the high viscosity of this polymer is the main factor to control the dissolution rate³⁶. Therefore, the release rate of PX from the microparticles could be modulated by adjusting the ratios of polymer:drug in the formulation.

Figure 7 reports the dissolution profiles of microparticles containing Ae compared with those of Eu S100:PX microparticles. The moderate decrease of dissolution rate of PX by the inclusion of Ae in microparticles appears to be related to the gelation property of Ae. Because of the -OH groups on the microparticle surface, Ae can form a great number of hydrogen bonds with the dissolution medium, absorbing water on the particle surface⁴⁴.

Stability studies

It is well known that amorphous drug formulations in the form of SDs tend to recrystallize on storage. Hence in this study, aging studies were performed. After 3 months of storage at 40°C/75% RH the dissolution profiles of microparticles were very similar to freshly prepared ones; moreover, no differences in

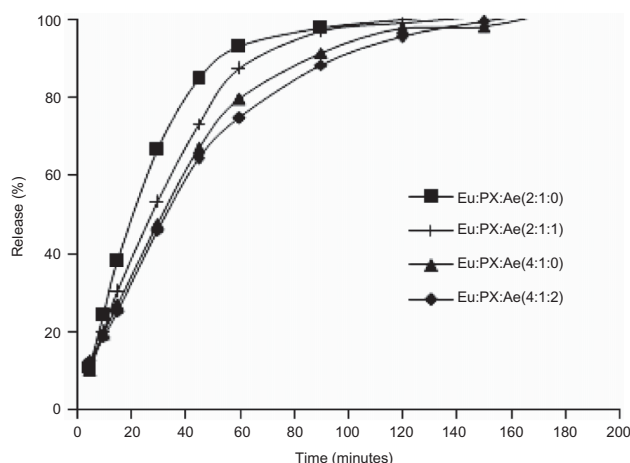


Figure 7. Release of PX from microparticles into pH 7.4 phosphate buffer from microparticles:Eu S100:PX:Ae at 2:1:0, 2:1:1, 4:1:0, and 4:1:2 ratios (\pm SD, $n = 3$).

the DSC curves were detected. These results, not shown for brevity, suggest the physical stability of the samples, at least for the examined time, which might be due to the hydrogen bonding between PX and Eu S100 in the microparticles.

Conclusion

PX microparticles having a SD structure were prepared successfully in one step using a spherical crystallization technique by combination with formation of SD. The preparation process was simple, reliable, and inexpensive; the resultant microparticles have the desired micromeritic properties. The release rate of PX from the microparticles could be modulated as desired by adjusting the formulations of the microparticles. The markedly improved dissolution rate of PX from the microparticles indicated that the present method was an efficient method for enhancing dissolution rate of water-insoluble drugs.

FTIR spectroscopy revealed possibility of H-bonding interaction between PX and Eu S100 in microparticles. The amorphous state of PX in the microparticles was kept even under severe conditions (40°C/75% RH) for 3 months, which might be because PX molecules have a H-bonding interaction with Eu S100.

Declaration of interest

The authors report no conflicts of interest. The authors alone are responsible for the content and writing of this paper.

References

- Dahl SL, Ward JR. (1982). Pharmacology, clinical efficacy, and adverse effects of piroxicam, a new nonsteroidal anti-inflammatory agent. *Pharmacotherapy*, 2:80–9.
- Mckellar QA, May SA, Lees P. (1991). Pharmacology and therapeutics of non-steroidal anti-inflammatory drugs in the dog and cat: 2 Individual agents. *J Small Anim Pract*, 32:225–35.
- Galbraith EA, Mckellar QA. (1991). Pharmacokinetics and pharmacodynamics of piroxicam in dogs. *Vet Rec*, 128:561–5.
- Streubel A, Siepmann J, Bodmeier R. (2006). Drug delivery to the upper small intestine window using gastroretentive technologies. *Curr Opin Pharmacol*, 6:501–8.
- Tanaka N, Imai K, Okimoto K, Ueda S, Tokunaga Y, Ibuki R, et al. (2006). Development of novel sustained-release system, disintegration-controlled matrix tablet (DCMT) with solid dispersion granules of nilvadipine (II): In vivo evaluation. *J Control Release*, 112:51–6.
- Leuner C, Dressman J. (2000). Improving drug solubility for oral delivery using solid dispersions. *Eur J Pharm Biopharm*, 50:47–60.
- Majerik V, Charbit G, Badens E, Horvath G, Szokonya L, Bosc N, et al. (2007). Bioavailability enhancement of an active substance by supercritical antisolvent precipitation. *J Supercrit Fluids*, 40:101–10.
- Prabhu S, Ortega M, Ma Ch. (2005). Novel lipid-based formulations enhancing the in vitro dissolution and permeability characteristics of a poorly water-soluble model drug, piroxicam. *Int J Pharm*, 301:209–16.
- Sumano H, Devizcaya A. (1996). Tolerance and clinical evaluation of piroxicam in dogs. *Canine Pract*, 21:16–9.
- Bjorkman DJ. (1996). Nonsteroidal anti-inflammatory drug-induced gastrointestinal injury. *Am J Med*, 101:S25–S32.
- Chiou WL, Riegelman S. (1970). Oral absorption of griseofulvin in dogs: Increased absorption via solid dispersion in polyethylene glycol 6000. *J Pharm Sci*, 59:937–42.
- Sekiguchi K, Obi N. (1961). Studies on absorption of eutectic mixture. I. A comparison of the behavior of eutectic mixture of sulfathiazole and that of ordinary sulfathiazole in man. *Chem Pharm Bull*, 9:866–72.
- Goldberg AH, Gibaldi M, Kamig JL. (1965). Increasing dissolution rates and gastrointestinal absorption of drugs via solid solutions and eutectic mixtures. I. Theoretical considerations and discussion of the literature. *J Pharm Sci*, 54:1145–8.
- Chiou WL, Riegelman S. (1971). Pharmaceutical applications of solid dispersion systems. *J Pharm Sci*, 60:1281–302.
- Ford JL. (1986). The current status of solid dispersions. *Pharm Acta Helv*, 61:69–88.
- Kawashima Y, Okumura M, Takenaka H. (1982). Spherical crystallization: Direct spherical agglomeration of salicylic acid crystals during crystallization. *Science*, 216:1127–8.
- Kawashima Y, Imai M, Takeuchi H, Yamamoto H, Kamiya K, Hino T. (2003). Improved flowability and compactibility of spherically agglomerated crystals of ascorbic acid for direct tableting designed by spherical crystallization process. *Powder Technol*, 130:283–9.
- Maghsoodi M, Hassan-zadeh D, Barzegar-jalali M, Nokhodchi A, Martin G. (2007). Improved compaction and packing properties of naproxen agglomerated crystals obtained by spherical crystallization technique. *Drug Dev Ind Pharm*, 33:1216–24.
- Cui FD, Kawashima Y, Takeuchi H, Niwa T, Hino T. (1996). Preparation of controlled releasing acrylic polymer microparticles of acebutolol hydrochloride and microparticles with sodium alginate in a polymeric spherical crystallization system. *Chem Pharm Bull*, 44:837–42.
- Maghsoodi M, Esfahani M. (2009). Preparation of microparticles of naproxen with Eudragit RS and Talc by spherical crystallization technique. *Pharm Dev Technol*, 14(4):442–50.
- Niwa T, Takeuchi H, Hino T, Itoh A, Kawashima Y, Kiuchi K. (1994). Preparation of agglomerated crystals for direct tableting and microencapsulation by the spherical crystallization technique with a continuous system. *Pharm Res*, 11:478–84.

22. Kawashima Y, Niwa T, Takeuchi H, Hino T, Itoh Y. (1991). Preparation of multiple unit hollow microparticles (microballoons) with acrylic resin containing tranilast and their drug release characteristics (in vitro) and floating behavior (in vitro). *J Control Release*, 16:279–90.
23. Niwa T, Takeuchi H, Hino T, Kunou N, Kawashima Y. (1993). Preparation of biodegradable nanospheres of water-soluble and insoluble drugs with DL-lactide/glycolide copolymer by a novel spontaneous emulsification solvent diffusion method and the drug release behavior. *J Control Release*, 25:89–98.
24. Kawashima Y. (1989). Spherical crystallization as a novel particle design technique for oral drug delivery system. *Chin Pharm J*, 41:163–72.
25. Cui FD, Wang X, Yang MS, Pang XJ. (2001). Studies on the preparation of sustained-release microparticles by spherical crystallization technique. In: *The 18th symposium on particulate preparations and designs*, Japan, 209–14.
26. Pilpel N. (1964). The flow properties of magnesia. *J Pharm Pharmacol*, 16:705–16.
27. Carr RL. (1965). Evaluation flow properties of solids. *Chem Eng*, 72:163–8.
28. Carr RL. (1965). Classify flow properties of solids. *Chem Eng*, 72:69–72.
29. Re MI, Biscans B. (1999). Preparation of microparticles of Ketoprofen with acrylic polymers by a quasi-emulsion solvent diffusion method. *Powder Technol*, 101:120–33.
30. Kachrimanis K, Nikolakakis I, Malamataris S. (2000). Spherical crystal agglomeration of ibuprofen by the solvent-change technique in presence of methacrylic polymers. *J Pharm Sci*, 89(2):250–8.
31. Zaniboni HC, Fell JT, Collett JH. (1995). Production and characterization of enteric beads. *Int J Pharm*, 125:151–5.
32. Thomopson CJ, Hansford D, Higgin S, Rostron C, Hutcheon CA, Munday DL. (2007). Evaluation of ibuprofen-loaded microparticles prepared from novel copolyesters. *Int J Pharm*, 329:53–61.
33. Yang MS, Cui F, You B, Fan Y, Wang L, Yue P, et al. (2003). Preparation of sustained-release nitrendipine microparticles with Eudragit RS and Aerosil using quasi-emulsion solvent diffusion method. *Int J Pharm*, 259:103–13.
34. Kawashima Y, Niwa T, Takeuchi H, Hino T, Itoh Y. (1992). Hollow microparticles for use as a floating controlled drug delivery system in the stomach. *J Pharm Sci*, 81(2):135–40.
35. Gennaro AR. (1990). *Remington's pharmaceutical sciences*. XVIII ed. Easton, PA: Mack Publishing Company, 1116.
36. Tantishaiyakul V, Kaewnopparat N, Ingkatawornwong S. (1999). Properties of solid dispersions of piroxicam in polyvinylpyrrolidone. *Int J Pharm*, 181:143–51.
37. Mihalic M. (1986). Piroxicam. In: Florey, K, ed. *Analytical profiles of drug substances*, vol. 15. London: Academic Press, 509–31.
38. Vrečer F, Vrbinc M, Meden A. (2003). Characterization of piroxicam crystal modifications. *Int J Pharm*, 256:3–15.
39. Gao Y, Cui F, Guan Y, Yang L, Wang Y, Zhang L. (2006). Preparation of roxithromycin-polymeric microparticles by the emulsion solvent diffusion method for taste masking. *Int J Pharm*, 318:62–9.
40. Tantishaiyakul V, Kaewnopparat N, Ingkatawornwong S. (1996). Properties of solid dispersions of piroxicam in polyvinylpyrrolidone K-30. *Int J Pharm*, 143:59–66.
41. Broman E, Khoo C, Taylor LS. (2001). A comparison of alternative polymer excipients and processing methods for making solid dispersions of a poorly water-soluble drug. *Int J Pharm*, 222:139–51.
42. Dordunoo SK, Ford JL, Rubinstein MH. (1991). Preformulation studies on solid dispersions containing triamterene or temazepam in polyethylene glycols or Gelucire 44/14 for liquid filling of hard gelatin capsules. *Drug Dev Ind Pharm*, 17:1685–713.
43. Passerini N, Perissutti B, Moneghini M, Voinovich D, Albertini B, Cavallari C, et al. (2002). Characterization of carmazepine/gelucire 50/13 microparticles prepared by a spray-congealing process using ultrasounds. *J Pharm Sci*, 91:699–707.
44. Albertinia B, Passerini N, González-Rodríguez ML, Perissutti B, Rodríguez L. (2004). Effect of Aerosil on the properties of lipid controlled release microparticles. *J Control Release*, 100:233–46.

Copyright of Drug Development & Industrial Pharmacy is the property of Taylor & Francis Ltd and its content may not be copied or emailed to multiple sites or posted to a listserv without the copyright holder's express written permission. However, users may print, download, or email articles for individual use.